CYLINDRICAL DIELECTRIC WAVEGUIDE MODES

by

Elias Snitzer

RESEARCH CENTER

American Optical COMPANY

Southbridge, Massachusetts

Scientific Report No. 1
Contract: AF19(604)7207

April, 1961

Prepared for

ELECTRONICS RESEARCH DIRECTORATE

AIR FORCE CAMBRIDGE RESEARCH LABORATORIES

OFFICE OF AEROSPACE RESEARCH

UNITED STATES AIR FORCE

BEDFORD, MASSACHUSETTS

AFCRL - 196

CYLINDRICAL DIELECTRIC WAVEGUIDE MODES

by

Elias Snitzer

RESEARCH CENTER
AMERICAN OPTICAL COMPANY
SOUTHBRIDGE, MASSACHUSETTS

Scientific Report No. 1

Contract: AF19(604)7207

April, 1961

Prepared for
Electronics Research Directorate
Air Force Cambridge Research Laboratories
Office of Aerospace Research
United States Air Force
Bedford, Massachusetts

Requests for additional copies by Agencies of the Department of Defense, their contractors, and other Government agencies should be directed to the:

Armed Services Technical Information Center
Arlington Hall Station
Arlington 12, Virginia

All other persons and organizations should apply to the:

U. S. Department of Commerce
Office of Technical Services
Washington 25, D. C.

ACKNOWLEDGEMENTS

The author gratefully acknowledges helpful discussions with Professor L. Chu of M.I.T., Professor S. P. Schlesinger of Columbia University, and Mr. J. W. Hicks of Mosaic Fabrications, Southbridge, Massachusetts.

ABSTRACT

The propagation of cylindrical dielectric waveguide modes near cut-off and far from cut-off are considered. The relative amounts of E_z and H_z, and the transverse components of the field are determined for both sets of hybrid modes. With the radial dependence of the z-components of the field in the central dielectric given by $J_n(ur/a)$, the transverse components far from cut-off are given by $J_{n\pm1}(ur/a)$, where u is a parameter found from the boundary conditions and which fixes the scale of the Bessel function relative to the boundary r=a. The two values n+1 and n-1 correspond to the two sets of modes. The designation of the hybrid modes are discussed. Field plots for the lower order modes are given.

TABLE OF CONTENTS

Cylindrical Dielectric Waveguide Modes

LIST OF ILLUSTRATIONS

I. INTRODUCTION

In a light pipe electromagnetic energy is propagated down the pipe by reflection from the walls of the structure. If the transverse dimensions are comparable to the wavelength of the light, only certain field distributions, or modes, will satisfy Maxwell's equations and the boundary conditions. In this case the light pipe is more appropriately considered as a waveguide. Even in very large structures there are waveguide modes, but there are so many of them, their number increasing as the area, that in most cases a geometrical optics description is more fruitful.

Waveguides were first dealt with by Lord Rayleigh.[1] Later the dielectric waveguide was investigated theoretically by Hondros and Debye[2] and experimentally by Schriever.[3]

The distinction between metallic and dielectric waveguides is in the reflection mechanism responsible for confining the energy. The metallic guide does so by reflection from a good conductor at the boundary. In the dielectric waveguide, this is accomplished by total internal reflection, which is gotten by having the central dielectric made of a material of higher index of refraction than the surrounding dielectric. The two regions will henceforth be referred to as the core and cladding.

In a metallic guide there are two sets of solutions, the transverse electric and transverse magnetic modes. In the dielectric guide all but the cylindrically symmetric modes, TE_{om} and TM_{om}, are hybrid, i.e. they have both electric and magnetic z-components.[4,5] In general, one would expect two sets of such hybrid modes, because the boundary conditions give a characteristic equation which is quadratic in the Bessel functions describing the field in the central dielectric. Beam et al[6] gave the two sets for n=1, and Abele[7] arrived at the two sets by a graphical solution of the characteristic equation.

Until recently the main concern has been with the three lowest order modes, HE_{11}, TE_{01} and TM_{01}. However, with the increased interest in end-fire antennas and the observations of waveguide modes in the visible region of the spectrum,[8] the higher order modes assume greater importance.

In this paper the two sets of solutions are given, including cut-offs, field distributions, and conditions far from cut-off. The designations of the hybrid modes are considered. Some properties of the propagating modes are discussed.

II. BASIC EQUATIONS

The cylindrical dielectric waveguide consists of a core of high dielectric constant ϵ_1 and radius a surrounded by a cladding of lower dielectric constant ϵ_2. Both regions are assumed to be perfect insulators with the free space magnetic permeability μ. Such a structure can have an infinite number of modes, but for given values of ϵ_1, ϵ_2 and a, only a finite number of these are waveguide modes have their fields localized in the vicinity of the core. The other "unbound" modes would correspond for example to light striking the core from the side, passing on through the core and emerging from the other side.

Choose a cylindrical coordinate system r, θ, z with the z-axis lying along the guide axis. A waveguide mode is a coherent distribution of light, localized in the vicinity of the core by total internal reflection, and which propagates down the guide with a well defined phase velocity. That is the z and time dependences are given by $\exp\left\{i(hz-\omega t)\right\}$, where w is the angular frequency and h is the propagation constant which is determined from the boundary conditions.

Because of the cylindrical symmetry, the other components of the field can be expressed in terms of E_z and H_z.[9] The z-components of the field satisfy the wave equation in cylindrical coordinates. The solutions are:

$$E_z = A_n J_n (\lambda_1 r) \cos (n\theta + \varphi_n) \exp \left\{ i(hz-\omega t) \right\} , \tag{1}$$

$$H_z = B_n J_n (\lambda_1 r) \cos (n\theta + \psi_n) \exp \left\{ i(hz-\omega t) \right\} . \tag{2}$$

The field in the cladding is given by replacing the constants A_n and B_n by C_n and D_n, and by replacing the Bessel function $J_n (\lambda_1 r)$ by the modified Hankel function of the first kind $K_n (\lambda_2 r)$. These particular Hankel functions are required in the cladding, because they are the only cylindrical functions that vanish sufficiently rapidly as r increases to infinity to describe a field bound to the central dielectric. With the definition of the propagation constant $k^2 = \omega^2 \mu \epsilon$, the λ's are defined by

$$\lambda_1^2 = k_1^2 - h^2, \quad \lambda_2^2 = h^2 - k_2^2; \tag{3}$$

both are real. φ_n and ψ_n are phase factors, which are related by the boundary conditions.

The transverse components of the field can be expressed in terms of E_z and H_z by[9]

$$E_r = i \frac{h}{k^2-h^2} \left[\frac{\partial E_z}{\partial r} + \frac{\mu\omega}{h} \frac{1}{r} \frac{\partial H_z}{\partial \theta} \right] \tag{4}$$

$$E_\theta = i \frac{h}{k^2-h^2} \left[\frac{1}{r} \frac{\partial E_z}{\partial \theta} - \frac{\mu\omega}{h} \frac{\partial H_z}{\partial r} \right] \tag{5}$$

$$H_r = i \frac{h}{k^2-h^2} \left[-\frac{k^2}{\mu\omega h} \frac{1}{r} \frac{\partial E_z}{\partial \theta} + \frac{\partial H_z}{\partial r} \right] \tag{6}$$

$$H_\theta = i \frac{h}{k^2-h^2} \left[\frac{k^2}{\mu\omega h} \frac{\partial E_z}{\partial r} + \frac{1}{r} \frac{\partial H_z}{\partial \theta} \right] \tag{7}$$

At the boundary r = a, the continuity of the tangential components of the field give the following four equations for the constants A_n, B_n, C_n, D_n. For simplicity $\lambda_1 a$ and $\lambda_2 a$ have been replaced by u and w. The continuity of the tangential components of E give

$$A_n J_n = C_n K_n, \tag{8}$$

$$A_n \frac{nh}{u^2} J_n \sin(n\theta + \varphi n) + B_n \frac{\mu\omega}{u} J_n' \cos(n\theta + \psi n) \tag{9}$$

$$= -C_n \frac{nh}{w^2} K_n \sin(n\theta + \varphi n) - D_n \frac{\mu\omega}{w} K_n \cos(n\theta + \chi n),$$

and from the tangential components of H,

$$B_n J_n = D_n K_n, \tag{10}$$

$$A_n \frac{k_1^2}{\mu\omega u} J_n' \cos(n\theta + \varphi n) - B_n \frac{nh}{u^2} J_n \sin(n\theta + \psi n)$$

$$= -C_n \frac{k_2^2}{\mu\omega w} K_n' \cos(n\theta + \varphi n) + D_n \frac{nh}{w^2} K_n \sin(n\theta + \chi n) \tag{11}$$

The primes on J_n and K_n refer to differentiation with respect to their arguments, u and w, respectively. Further, define n_1 and n_2 by

$$n_1 = \frac{J_n'(u)}{u J_n(u)}, \quad n_2 = \frac{K_n'(w)}{w K_n(w)} \tag{12}$$

For the four equations to be consistent, the determinant of the coefficients must vanish, giving

$$\frac{(n_1 + n_2)(k_1^2 n_1 + k_2^2 n_2)}{n^2 h^2 (1/u^2 + 1/w^2)^2} = -\frac{\sin(n\theta + \varphi n) \sin(n\theta + \psi n)}{\cos(n\theta + \varphi n) \cos(n\theta + \chi n)} \tag{13}$$

The left side of (13) is independent of angle; therefore, the phases φ_n and χ_n must be related such as to make the right side a constant. This will be the case if

$$\chi_n - \varphi_n = \pm \pi/2. \tag{14}$$

Then (13) becomes

$$(n_1 + n_2)(k_1^2 n_1 + k_2^2 n_2) = n^2 h^2 (1/u^2 + 1/w^2)^2. \tag{15}$$

Eq. (15) together with Eqs. (3) determine the value of h. The quantity u enters (7) both explicitly and as the argument of n_1. However, n_1 is a rapidly varying oscillatory function of u. Hence, (15) can be considered roughly as a quadratic equation in n_1. The two sets of solutions are the two sets of hybrid modes.

From the set of four boundary condition equations, the relative amounts of E_z and H_z in a hybrid mode can be found in a straightforward way. The result is

$$P = \frac{\mu\omega}{h} \frac{B_n}{A_n} \frac{\cos(n\theta + \chi_n)}{\sin(n\theta + \varphi_n)} = \frac{n(1/u^2 + 1/w^2)}{n_1 + n_2} \tag{16}$$

The coefficient $\mu\omega/h$ in the definition of P has been included for convenience in later use.

Expressed in terms of P, the field in the core becomes

$$E_z = J_n(\lambda_1 r)\, F_c,$$

$$E_r = i\,\frac{h}{\lambda_1}\left[J_n^{1} - P\,\frac{nJn}{\lambda_1 r}\right] F_c,$$

$$E_\theta - i\,\frac{h}{\lambda_1}\left[PJ_n^{1} - \frac{nJn}{\lambda_1 r}\right] F_s,$$

$$H_z = -\frac{h}{\mu\omega}\, PJ_n\, F_s \qquad (17)$$

$$H_r = -i\,\frac{k_1^2}{\mu\omega\lambda_1}\left[P\,\frac{h^2}{k_1^2}\, J_n^{1} - \frac{nJn}{\lambda_1 r}\right] F_s,$$

$$H_\theta = i\,\frac{k_1^2}{\mu\omega\lambda_1}\left[J_n^{1} - P\,\frac{h^2}{k_1^2}\,\frac{nJ_n}{\lambda_1 r}\right] F_c.$$

The prime indicates differentiation with respect to the argument of the Bessel function and

$$F_c = A_n \cos(n\theta + \varphi_n) \exp\left\{i(hz-\omega t)\right\} \qquad (18)$$

$$F_s = A_n \sin(n\theta + \varphi_n) \exp\left\{i(hz-\omega t)\right\}.$$

III. THE CUT-OFF CONDITIONS

The cut-offs for the various modes are found by solving (15) in the limit of $w^2 \to 0$.

Define new quantities ξ_1 and ξ_2 by

$$\xi_1 = \frac{J_n - 1}{u\, J_n} \quad , \qquad \xi_2 = \frac{K_n - 1}{w\, K_n} \tag{19}$$

By using the Bessel and Hankel function identities, Eqs. (A4) and (A6) in the appendix, (15) can be rewritten as

$$\xi_1^2 - \xi_1 \left[\frac{K_1^2 + K_2^2}{K_1^2}\, \xi_2 + n\left(\frac{2}{u^2} + \frac{K_1^2 + K_2^2}{K_1^2}\, \frac{1}{w^2} \right) \right]$$

$$+ \left[\frac{K_2^2}{K_1^2}\, \xi_2^2 + \xi_2\, n \left(\frac{(K_1^2 + K_2^2)}{K_1^2}\, \frac{1}{u^2} + 2\, \frac{K_2^2}{K_1^2}\, \frac{1}{w^2} \right) \right] = 0 \tag{20}$$

ξ_1 is a function of u, but as pointed out earlier, ξ_1 varies so much more rapidly than u that where u appears explicitly in (20) it can be considered a constant. The two sets of cut-off values for different n can be obtained by substituting for the limit of $w^2 \to 0$.

Consider first the case of $n \geq 2$. From Eq. (A10) as $w^2 \to 0$,

$$\xi_2 = 1/\left[2(n-1)\right] \quad . \tag{21}$$

The two sets of roots of (20) are

$$\xi_1 = \frac{1}{n-1}\, \frac{k_2^2}{k_1^2 + k_2^2} \, , \tag{22}$$

$$\xi_1 = n \frac{k_1^2 + k_2^2}{k_1^2} \quad \frac{1}{w^2} \to \infty \tag{23}$$

Eq. (23) is equivalent to $J_n(u)=0$.

The cut-off values from (22) are given by Schelkunoff.[5] Those from (23) were found by Abele[9] by a graphical solution of equation (15). Substituting for ξ_1 in terms of the Bessel functions and using (A1) with n replaced by (n-1) puts Eq. (22) in a more convenienc form for small differences in dielectric constant between core and cladding. The result is

$$\frac{u\, J_{n-2}(u)}{J_{n-1}(u)} = -(n-1)\, \frac{\epsilon_1 - \epsilon_2}{\epsilon_2} . \tag{24}$$

For small differences in dielectric constant the cut-offs are given approximately by $J_{n-2}(u) = 0$. For n=2, this gives another set of modes whose cut-offs are close to the TE_{om} and TM_{om} modes. The interesting effects this has on optical waveguide modes are discussed in a companion article in this journal.

For n=1, from Eq. (A9) in the limit of $w^2 \to 0$ the two roots of (20) are

$$\xi_1 = \frac{k_1^2 + k_2^2}{k_1^2} \quad \frac{1}{w^2} \to \infty \tag{25}$$

$$\xi_1 = \frac{2\, k_2^2}{k_1^2 + k_2^2} \quad \ln \frac{2}{\gamma w} \to \infty \tag{26}$$

Both of the above equations have cut-offs given by

$$J_1 (u)=0 \tag{27}$$

The root of Eq. (27) at u=0 corresponds to the well-known HE_{11} mode which does not have a cut-off.

Eq. (27) specifies two sets of modes whose cut-off conditions are identical. However, the HE_{11} mode is the first mode of only one of the sets. This is because $1/u^2$ in equation (20) cannot be considered as slowly varying near u=0. In fact, ξ_1 becomes $2/u^2$ near u=0 and the quadratic term ξ_1^2, drops out of the equation.

The relative amounts of E_Z and H_Z in the hybrid modes can be found by substituting in Eq. (16) the limiting values of ξ_1 and ξ_2 as w→0. The results together with the cut-off conditions are summarized in Table I.

Let u_{nm} be the value u assumes at cut-off for the m'th root of the cut-off condition involving the n'th order Bessel function. The possible values of u_{nm} are the roots of the equations giving the cut-off conditions in Table I. At cut-off, w=0 and h=k_2; hence, the first of Eqs. (3) becomes

$$u_{nm} = 2\pi (a/\lambda) \ (n_1^2 - n_2^2)^{1/2} , \tag{28}$$

where λ is the free space wavelength and n_1 and n_2 are the indices of refraction of core and cladding, respectively.

The modes which can propagate are those for which u_{nm} are less than $2\pi (a/\lambda) \ (n_1^2 - n_2^2)^{1/2}$. Since u_{nm} forms

an increasing sequence for fixed n and increasing m or for fixed m and increasing n, the number of allowed modes increases as the square of the radius a.

IV. CONDITIONS FAR FROM CUT-OFF

The field in a mode far from cut-off can be found in the same way as that near cut-off. Only now the asymptotic forms for large w are substituted for ζ_2 in Eq. (20). Table II summarizes the conditions far from cut-off.

V. MODE DESIGNATIONS

For cylindrical metallic waveguides the modes are designated TE_{nm} and TM_{nm}, or in the older literature these were H_{nm} and E_{nm} modes, respectively. The transverse electric mode TE_{nm} can be derived from a single field quantity, the z-component of the magnetic field, hence the alternative designation H_{nm} for this mode.

In the dielectric waveguide only the cylindrically symmetric n = 0 modes are either transverse electric (TE_{om}) or transverse magnetic (TM_{om}). The other modes are hybrid, i.e. they have non-zero values for both E_z and H_z.

Following Wegner, [10] Beam[6] suggested a scheme for the designation of the hybrid modes based on the relative

contributions of E_z and H_z to a transverse component of the field at some reference point. If E_z makes the larger contribution, the mode is considered E-like and designated EH_{nm}, etc. This method of designation is arbitrary, for it does depend on the particular transverse component of the field chosen, the reference point, and how far the wavelength is from cut-off. However, the use of two letters, such as EH and HE, to designate the hybrid modes is reasonable because it does imply the hybrid nature of these modes.

It has become common usage in the microwave literature to refer to the mode without a cut-off as the HE_{11} mode. Referring to Table II, it is seen that this mode has a value of P = -1 far from cut-off. It is proposed that all the modes with P = -1 be designated HE_{nm} and the modes with P = +1 be designated EH_{nm}. The basic physical difference between the HE and EH modes will be discussed later in the section on field plots.

The subscripts on HE_{nm} or EH_{nm} refer to the n'th order and m'th rank, where the rank gives the successive solutions of the boundary condition equation involving J_n. It is customary to label these solutions in order starting from m = 1; this procedure is followed here. Notice that this makes the cut-off parameters for the HE_{12} and EH_{11} mode the same, namely the [illegible]t of $J_1(u)=0$ at u=3.832. Table I summarizes the mode designations suggested here.

VI. THE TRANSVERSE COMPONENTS OF THE FIELD

By use of Eqs. (A1), (A2) and (17) the field in the core can be written as

$$
\begin{aligned}
E_z &= J_n(\lambda_1 r)\, F_c, \\
E_r &= i\frac{h}{\lambda_1}\left[\frac{1-P}{2} J_{n-1} \quad \frac{1+P}{2} J_{n+1}\right] F_c, \\
E_\theta &= i\frac{h}{\lambda_1}\left[-\frac{1-P}{2} J_{n-1} \quad \frac{1+P}{2} J_{n+1}\right] F_s, \\
H_z &= -\frac{h}{\mu\omega} P J_n F_s, \\
H_r &= -i\frac{k_1^2}{\mu\omega\lambda_1}\left[-\frac{1-Ph^2/k_1^2}{2} J_{n-1} - \frac{1+Ph^2/k_1^2}{2} J_{n+1}\right] F_s, \\
H_\theta &= i\frac{k_1^2}{\mu\omega\lambda_1}\left[\frac{1-Ph^2/k_1^2}{2} J_{n-1} - \frac{1+Ph^2/k_1^2}{2} J_{n+1}\right] F_c,
\end{aligned}
\tag{29}
$$

The quantities F_c and F_s continue to be given by Eqs. (18).

For small differences in refractive index between the core and cladding $k_1^2/k_2^2 \cong 1$, $h^2/k_1^2 \cong 1$ and from Tables I and II $P = \pm 1$. The value $P = +1$ is for the EH modes and $P = -1$ goes with the HE modes. It is seen from Eqs. (29) that the transvers components of the field depend on r through J_{n+1} for the EH modes and have a dependence of J_{n-1} for the HE modes.

VII. ENERGY FLOW

The energy flow per unit area as a function of r and θ is given by the real part of the complex Poynting vector, $\underset{\sim}{S}^* = 1/2\ \underset{\sim}{E} \times \underset{\sim}{\tilde{H}}$, where $\underset{\sim}{\tilde{H}}$ is the complex conjugate of $\underset{\sim}{H}$. Only the z-component of $\underset{\sim}{S}^*$ is real and the power per unit area is given by

$$S_z = 1/2\ (E_r H_\theta - E_\theta H_r). \tag{30}$$

Substitution from Eqs. (29) gives after some simplification

$$S_z = \frac{1}{2} \frac{h}{\mu\omega} \frac{k_1^2}{\lambda_1^2} A_n^2 \left[\frac{(1-P)\ (1-Ph^2/k_1^2)}{4} J_{n-1}^2 + \frac{(1+P)\ (1+Pn^2/k_1^2)}{4} J_{n+1}^2 - \frac{1-P^2h^2/k_1^2}{2} J_{n-1}\ J_{n+1} \cos 2(n\theta + \varphi_n) \right] \tag{31}$$

For small index differences $P = \pm 1$ and the term containing θ drops out. The energy flow is then nearly circularly symmetrical with a radial dependence of

$$S_z \propto J_{n\mp1}^{\ 2} \tag{32}$$

The upper sign n-1 is for the HE modes and the lower for EH.

VIII. CHARACTERISTICS OF PROPAGATING MODES

For a waveguide mode λ_1 and λ_2 must both be real. Hence from Eq. (3)

$$k_2^2 \leq h^2 \leq k_1^2. \tag{33}$$

A guide wavelength λ_g, phase velocity v_{ph} and effective refractive index n_{eff} can be defined for a mode at the free space wavelength λ by

$$\omega/h = v_{ph} = \nu\lambda_g = c/n_{eff}, \tag{34}$$

where c is the velocity of light in vacuum. With (34) and the definition of the k's, Eq. (33) becomes

$$c/n_1 \leq v_{ph} \leq c/n_2 \tag{35}$$

That is, the phase velocity is intermediate between the velocities of propagation in bulk material of which the core and the cladding are made. At cut-off $h=k_2$ or

$$v_{ph} = c/n_2. \tag{36}$$

Far from cut-off the other equality in (35) holds.

Eq. (36) is the physical optics analogue of the geometrical optics condition that propagation in the light pipe occurs when the angle of incidence on the boundary exceeds the critical angle for total internal reflection. Consider a plane wave incident on the side of the core as shown in figure 1. The wave normal is in the direction $\underset{\sim}{p}$, and S_1 and S_2 are two

equiphase surfaces separated by λ/n_1, the wavelength in a homogeneous medium of refractive index n_1. The apparent wavelength along the guide, λg, is given by

$$\lambda g = \lambda/n_1 \sin \alpha \ . \qquad (37)$$

But Snell's law gives for the critical angle for total internal reflection, $n_2 = n_1 \sin \alpha$. Hence at cut-off (37) becomes $\lambda g = \lambda/n_2$, or $v_{ph} = c/n_2$, which is the same as Eq. (36).

Fig. 2 gives the very useful plot of frequency versus the inverse of the guide wavelength, that is c/λ vs. $1/\lambda g$ for the propagating modes. To obtain these curves, Eqs. (3) and (15) are solved for h as a function of λ and the parameters of the guide for each propagating mode. The mode lines shown in Fig. 2 are only schematic. A number of machine computations of these lines are available in the literature for the HE_{11} and TE_{01} modes,[6,11]

Propagation in the modes is such as to be confined to the region between the lines whose slopes are c/n_1 and c/n_2. Each mode as a function of wavelength is represented by a line which approaches the c/n_1 line far from cut-off and terminates at the c/n_2 line at cut-off. All the modes which have cut-offs terminate sharply at the c/n_2 line, but the HE_{11} mode, which does not have a cut-off, approaches the c/n_2 line slowly, finally merging with it at the origin. The number of modes increases as the square of the frequency.

The significance of a mode line can best be understood by a specific example. Consider the TE_{01} mode excited at the frequency ν'. Then $1/\lambda_g$ is the coordinate of the intersection of the TE_{01} line with the ordinate ν'. The slope of the line connecting this point with the origin is $c/n_{01}(\lambda)$, where $n_{01}(\lambda)$ is the effective index of refraction of the TE_{01} mode excited at the free space wavelength λ. $c/n_{01}(\lambda)$ is the phase velocity, whereas the slope of the mode curve at ν' is the group velocity.

IX. FIELD PLOTS

The field distribution can be given in the usual way by field lines in which the direction of the line at a point gives the direction of the field and the density of lines its magnitude. Only the field in the core will be considered. The field in the cladding can be inferred from the boundary conditions which require that the tangential components of $\underset{\sim}{E}$ and $\underset{\sim}{H}$, and the normal components of $\epsilon\underset{\sim}{E}$ and $\mu\underset{\sim}{H}$ be continuous. Since the field components in the cladding depend on modified Hankel function which monotonously go to zero with increasing r, the density of field smoothly decreases with an increase in the radial coordinate.

In Fig. 3 is shown the field distribution in the core for the TE_{02} mode far from cut-off. The field components from which Fig. 3 was sketched are given in Eqs. (17) or (29). The distribution is the instantaneous values in a transverse plane and in two longitudinal half planes of length $\lambda_g/2$ in the z-direction. In the transverse plane the magnetic field lines shown do not form closed curves; this is done to imply that these field lines close by going down the z-direction. The dots and crosses in the longitudinal planes specified that the electric field is perpendicular to these planes. The field line enters the plane at a dot and leaves it at a cross.

The z-component of the magnetic field varies as $J_o(u\ r/a)$. From Table II far from cut-off u is the second zero of $J_1(u) = 0$ or $u = 7.02$, and at cut-off u is the second zero of $J_0(u) = 0$ or $u = 5.52$. Hence, as the cut-off wavelength is approached the field distribution in the core readjusts itself so as to make the boundary of the core shift from the value $u = 7.02$ shown in Fig. 3 to the value $u = 5.52$.

For the TE_{01} mode the boundary $r = a$ is at $\mu = 3.83$ far from cut-off and at $\mu = 2.41$ at cut-off. The field distribution for the TM_{02} mode is obtained from Fig. 3 simply by interchanging the roles of E and H.

Since the Poynting vector is a function of the vector product of the transverse components of the field, it is clear from Fig. 3 that an image of the intensity distribution in the TE_{02} or TM_{02} modes should consist of two concentric circles.

It is interesting to compare the field distribution for the TE_{om} and TM_{om} modes with that obtained for the metallic waveguide.[12] In the later case the electric field is normal to the metallic boundary surrounding the core and the magnetic field is parallel to it. Hence, the metallic TE_{om} modes look like the dielectric TE_{om} far from cut-off, but the metallic TM_{om} modes have the field distrubition of the dielectric TM_{om} modes at cut-off.

For the hybrid modes ($n \geq 1$) the field distribution simplifies considerably for the case of a small index difference between the core and the cladding. From Eq. (29) for the z-components given by

$$(E_z, H_z) \propto J_n (ur/a) \cos n\theta, \tag{38}$$

the transverse components of the electric field are

$$E_r \propto (\pm 1) J_{n\pm 1} (u\, r/a) \cos n\theta, \tag{39}$$

$$E_\theta \propto J_{n\pm 1} (u\, r/a) \sin n\theta. \tag{40}$$

The proportionality constants are the same for E_r and E_θ. The plus sign is for the EH_{nm} modes and the minus sign for the HE_{nm} modes.

A given field line will be contained on a surface whose projection in the transverse r, θ plane is the solution of

$$\frac{dr}{r d\theta} = E_r/E_\theta \tag{41}$$

For a small difference in refractive indices between the core and the cladding Eqs. (39) and (40) apply, and the right side of (41) is a function of θ only. The result is

$$\frac{dr}{r\, d\theta} = \begin{matrix} + \\ - \end{matrix} \frac{\cos n\,\theta}{\sin n\,\theta}. \tag{42}$$

The above can be integrated to give

$$r = C (\sin n\,\theta) \pm 1/n, \tag{43}$$

where C is an integration constant. The plus sign in the exponent is for the EH_{nm} modes and the minus sign for the HE_{nm} modes. By assigning different values to C a family of curves is obtained which gives the electric field in a transverse plane. The magnetic field can be found in the same way; it is the same as for the electric field but with the pattern rotated by $\pi/(2n)$.

For the HE_{1m} modes Eq. (43) becomes

$$r \sin \theta = \text{constant}.$$

This is the equation for a set of straight lines parallel to the x-axis. Fig. 4 shows the field distribution for the HE_{12} mode. Far from cut-off the boundary of the core is at the second root of $J_o(u) = 0$ or $u = 5.52$ and at cut-off the boundary is at the zero of $J_1(u) = 0$ at $u = 3.83$. For the HE_{11} mode the boundary shifts from $u = 2.41$ for short wavelengths to $u = 0$ with increasing wavelength.

From Eq. (43) the electric field lines in a transverse plane for the EH_{11} mode satisfy

$$r = C \sin \theta, \tag{45}$$

or

$$x^2 + (y - C/2)^2 = C^2/4. \tag{46}$$

By assigning different values to C, Eq. (46) gives a set of circles that are all tangent to the x-axis at the origin. Fig. 5 gives the field plot for the EH_{11} mode. Far from cut-off the

boundary of the core is at the first zero of $J_2(u) = 0$ or $u = 5.14$ and at cut-off the boundary is at the first zero of $J_1(u) = 0$ at $u = 3.83$.

For the HE_{21} mode the electric field in a transverse plane is

$$r = C\ (\sin 2\theta)^{-1/2} \tag{47}$$

or

$$xy = \text{Constant}. \tag{48}$$

For various values of the constant Eq. (48) gives a set of hyperbolas. The field lines are shown in Fig. 6. Far from cut-off the boundary of the core is at the first root of $J_1(u) = 0$ or $u = 3.83$ and at cut-off the boundary is at a value of u somewhat larger than the first root of $J_o(u) = 0$ or $u = 2.41$.

To find a more precise value of u at cut-off for the case of a small index difference the left side of Eq. (24) can be expanded about the zero of $J_{n-2}(u) = 0$. To the first order terms the result is

$$u'_{nm} = u_{n-2,m} + \frac{n-1}{u_{n-2,m}} \quad \frac{n_1^2 - n_2^2}{n_2^2} \tag{49}$$

The prime on u'_{nm} indicates that it is the cut-off parameter for the HE_{nm} modes obtained from Eq. (24).

Where the field lines in Fig. 6 do not form closed curves but end in a plane, the field lines close by moving perpendicular to the indicated plane. The lower portion of Fig. 6 shows the closed contours for the electric field in a hyperbolic section bb'.

The field plots for the higher order modes are obtained in the same way as those above.

The EH_{nm} and HE_{nm} modes both have roughly the same r-dependences for (E_z, H_z), mainly $J_n(ur/a)$. But the transverse components depend on $J_{n+1}(ur/a)$ for the EH modes and on $J_{n-1}(ur/a)$ for the HE modes. This means that the field lines which are parallel to the guide axis at z=0 tend to form closed contours by going to larger radii in the region $0 < |z| < \lambda_g/4$ for the EH modes, but on the whole close by going to smaller radii for the HE modes. Hence, for the EH modes the peaks in the Poynting fluxare located further from the center of the guide than the peaks in E_z and H_z; the reverse is the case for the HE modes.

Table I. Summary of Cut-Off Conditions

The Bessel function of order n and argument u is given by $J_n(u)$, and ϵ_1 and ϵ_2 are the dielectric constants for core and cladding. P gives the relative amount of H_z to E_z in a mode (see text for exact definition).

	First Set of Solutions			Second Set of Solutions		
	Cut-off Condition	P at Cut-off	Suggested mode Designation	Cut-off Condition	P at Cut-off	Suggested Mode Designation
n=0	$J_o(u)=0$	0	TM_{om} m=1,2···	$J_o(u)=0$	∞	TE_{om} m=1, 2···
n=1	$J_1(u)=0$	-1	HE_{1m} m=1,2···		$\frac{k_1^2}{k_2^2}$	EH_{1m} m=1,2···
n≥2	$\frac{uJ_{n-2}(u)}{J_{n-1}(u)} = -(n-1)\frac{\epsilon_1-\epsilon_2}{2}$	-1	HE_{nm} m=1,2···	$J_n(u)=0$	$\frac{k_1^2}{k_2^2}$	EH_{nm} m=1,2···

Table II. Summary of Conditions Far from Cut-Off.

	First Solutions		Second Solutions	
	u	P	u	P
n=0	$J_1(u)=0$	0 (TM)	$J_1(u)=0$	∞ (TE)
n≥1	$J_{n-1}(u)=0$	-1 (HE)	$J_{n+1}(u)=0$	+1 (EH)

APPENDIX: PROPERTIES OF BESSEL AND HANKEL FUNCTIONS

The argument of the Bessel functions is u and of the modified Hankel functions w.

$$\frac{n\,J_n}{u} = \frac{1}{2}\quad (J_{n-1} + J_{n+1}), \tag{A1}$$

$$J_n' = \frac{1}{2}\quad (J_{n-1} - J_{n+1}), \tag{A2}$$

$$J_{-n} = (-1)^n\ J_n.$$

From the first two equations above

$$\frac{J_n'}{u\ J_n} = \frac{J_{n-1}}{u\ J_n} - \frac{n}{u^2} \tag{A4}$$

For w real the modified Hankel functions $K_n(w)$ are defined by

$$K_n(w) = \frac{\pi}{2}\ i^{\,n+1}\ H_n^{(1)}\ (iw), \tag{A5}$$

where $H_n^{(1)}$ (iw) are the Hankel functions of the first kind. The equation corresponding to (A4) is

$$\frac{K_n'}{w\ K_n} = \frac{K_{n-1}}{w\ K_n} + \frac{n}{w^2} \tag{A6}$$

For small w,

$$K_o(w) = \ln (2/\gamma w), \tag{A7}$$

$$K_n(w) = (n-1)!\, 2^{n-1}\, n^{-2} \text{ for } n \geq 1, \tag{A8}$$

where γ is Euler's constant and equal to 1.781. Still in the limit of w small,

$$\frac{K_o}{w\, K_1} = \ln (2/\gamma w), \tag{A9}$$

$$\frac{K_{n-1}}{w\, K_n} = \left[2(n-1)\right]^{-1} \text{ for } n \geq 2. \tag{A10}$$

The asymptotic expressions for large w are

$$K_n(w) = (\pi/2w)^{1/2} \exp\left\{-w\right\}, \tag{A11}$$

$$\frac{K_{n-1}}{w\, K_n} = \frac{1}{w}. \tag{A12}$$

CAPTIONS FOR FIGURES

Fig. 1 Construction to show the equivalence of the waveguide condition that at cut-off $v_{ph} = c/n_2$ with the geometrical optics conditions that propagation occurs only if the angle of incidence of the wave on the fiber wall exceeds the critical angle for total internal reflection. The wave normal is given by $\underset{\sim}{p}$, S_1 and S_2 are two equiphase surfaces separated by λ/n_1, and λ_g is the guide wavelength.

Fig. 2 Typical curves of the frequency ν versus $1/\lambda_g$ for mode propagation in a dielectric waveguide. Each mode is represented by a line which is confined to the region between the lines whose slopes are c/n_2 and c/n_1. At the frequency ν' the TE_{01} mode has a guide wavelength of λ_g', phase velocity v_{ph} and group velocity vgroup.

Fig. 3 Field plot in the core for the TE_{02} mode far from cut-off and for a small difference in indices of refraction of the core and cladding.

Fig. 4 Field plot in the core for the HE_{12} mode far from cut-off and for a small difference in indices of refraction of the core and cladding.

Fig. 5 Field plot in the core for the EH_{11} mode far from cut-off and for a small difference in indices of refraction of the core and cladding.

Fig. 6 Field plot in the core for the HE_{21} mode far from cut-off and for a small difference in indices of refraction of the core and cladding.

REFERENCES

1. Lord Rayleigh, Phil. Mag., 43, 125 (1897).

2. D. Hondros and P. Debye, Ann. Physik, 32, 465 (1910).

3. O. Schriever, Ann. Physik, 63, 645 (1920).

4. J. R. Corson, S.P. Mead, and S. A. Schelkunoff, Bell System Tech. J., 15, 310 (1936).

5. S. A. Schelkunoff, "Electromagnetic Waves" (D. Van Nostrand, Inc., New York, 1943), p. 425.

6. R. E. Beam, M. M. Astrahan, W. C. Jakes, H. M. Wachowski, and W. L. Firestone, Northwestern University Report ATI 94929, Chap. V (1949).

7. M. Abele, Nuovo Cimento 5, 274 (1948).

8. E. Snitzer and J. W. Hicks, J. Opt. Soc. Am., 49, 1128 (1959); H. Osterberg, E. Snitzer, M. Polanyi, R. Hilberg and J. W. Hicks, Ibid.

9. J. A. Stratton, "Electromagnetic Theory" (McGraw-Hill Book Co., Inc., New York, 1941), Chap. V.

10. H. Wegner, Air Material Command Microfilm ZWV/FB/RE/2018, R 8117F831.

11. S. P. Schlesinger and D. D. King, Trans. of the I.R.E., M.T.T. 6, 291 (1958).

12. J. F. Reintzes and G. T. Coate, "Principles of Radar" (McGraw-Hill Book Co., Inc. New York, 1952) 3rd. ed., Chap. 8, p. 609.

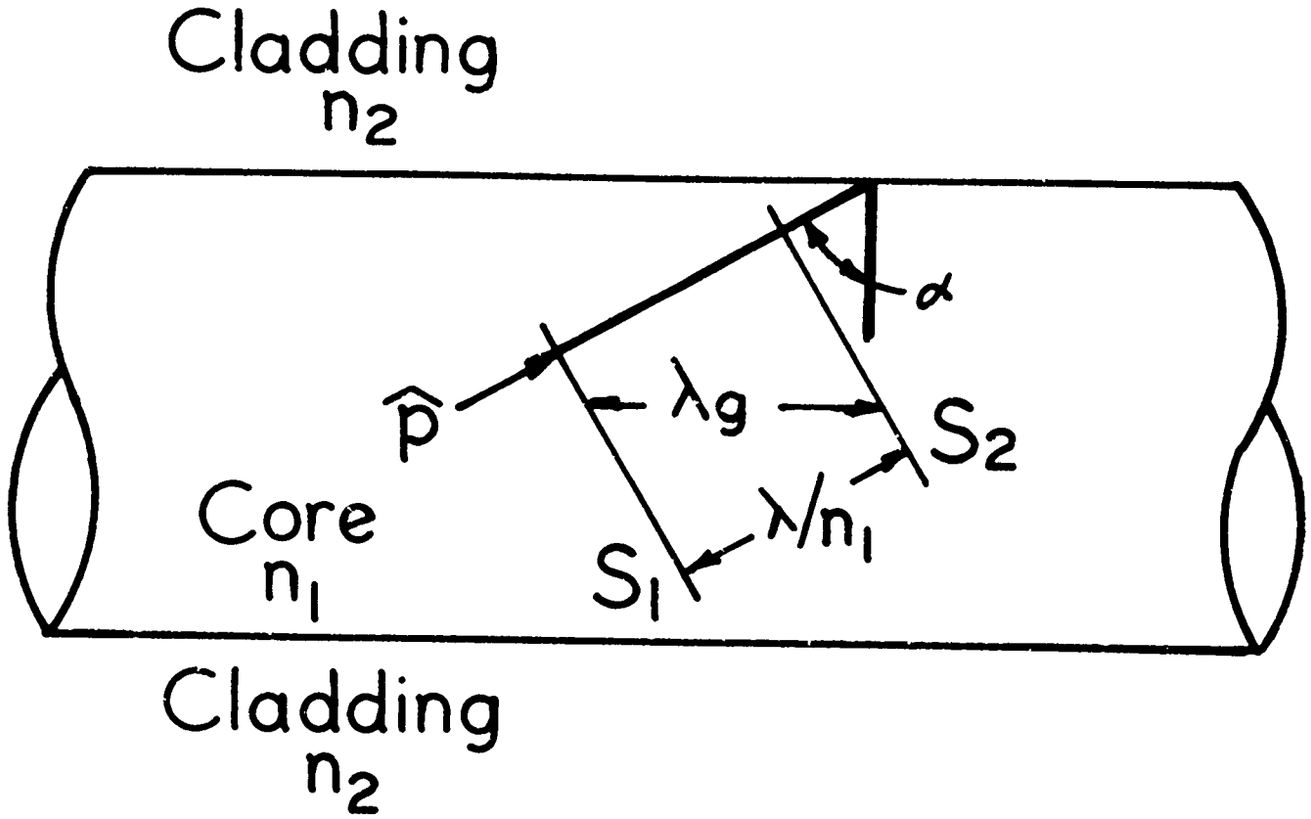
Cladding
n_2
α
$\hat{p}$
λ_g
S_2
λ/n_1
Core
n_1
S_1
Cladding
n_2

FIG. 1

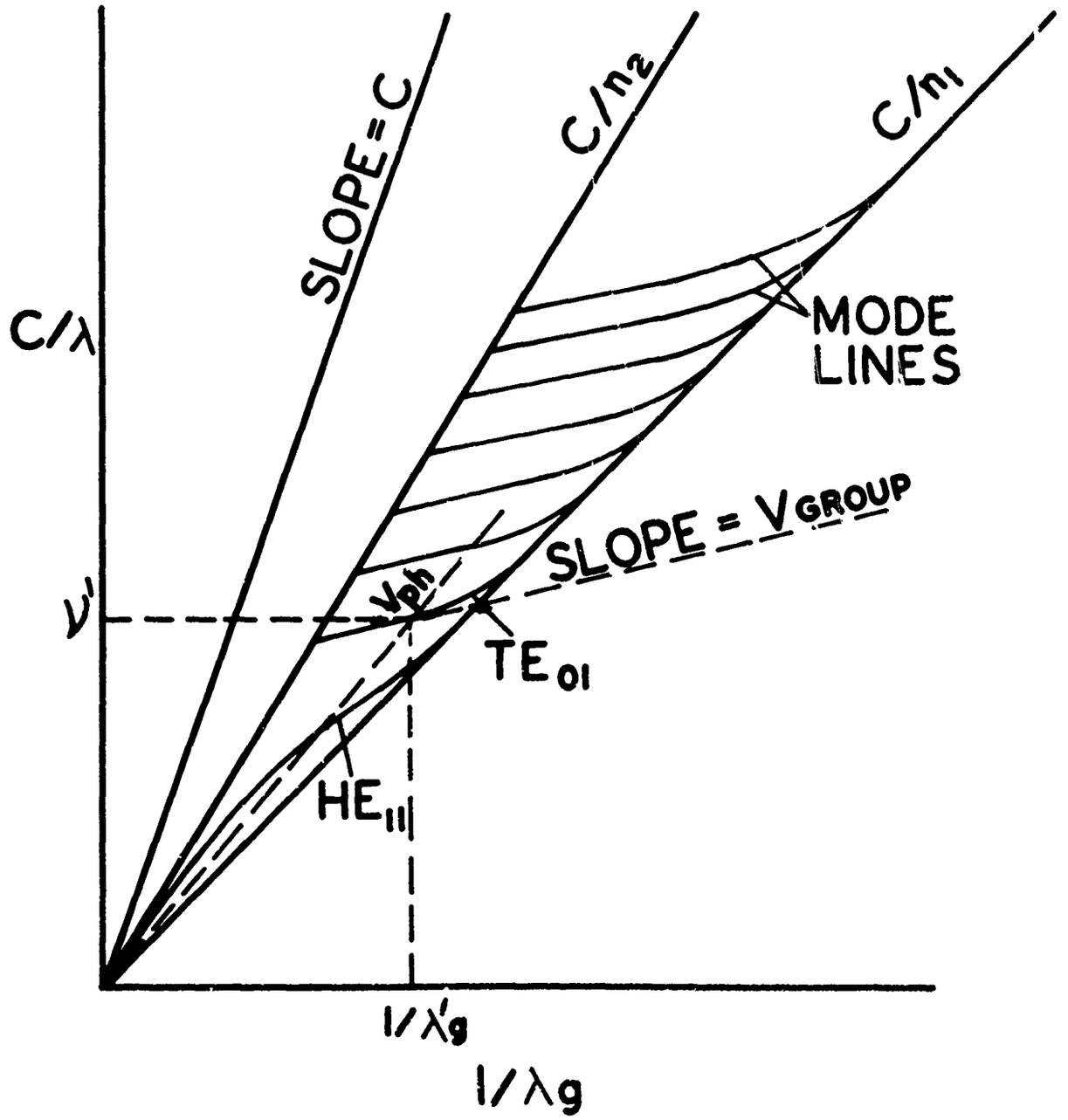
SLOPE=C
C/n2
C/n1
C/λ
MODE
LINES
SLOPE = VGROUP
ν'
Vph
TE01
HE11
1/λ'g
1/λg

FIG.2

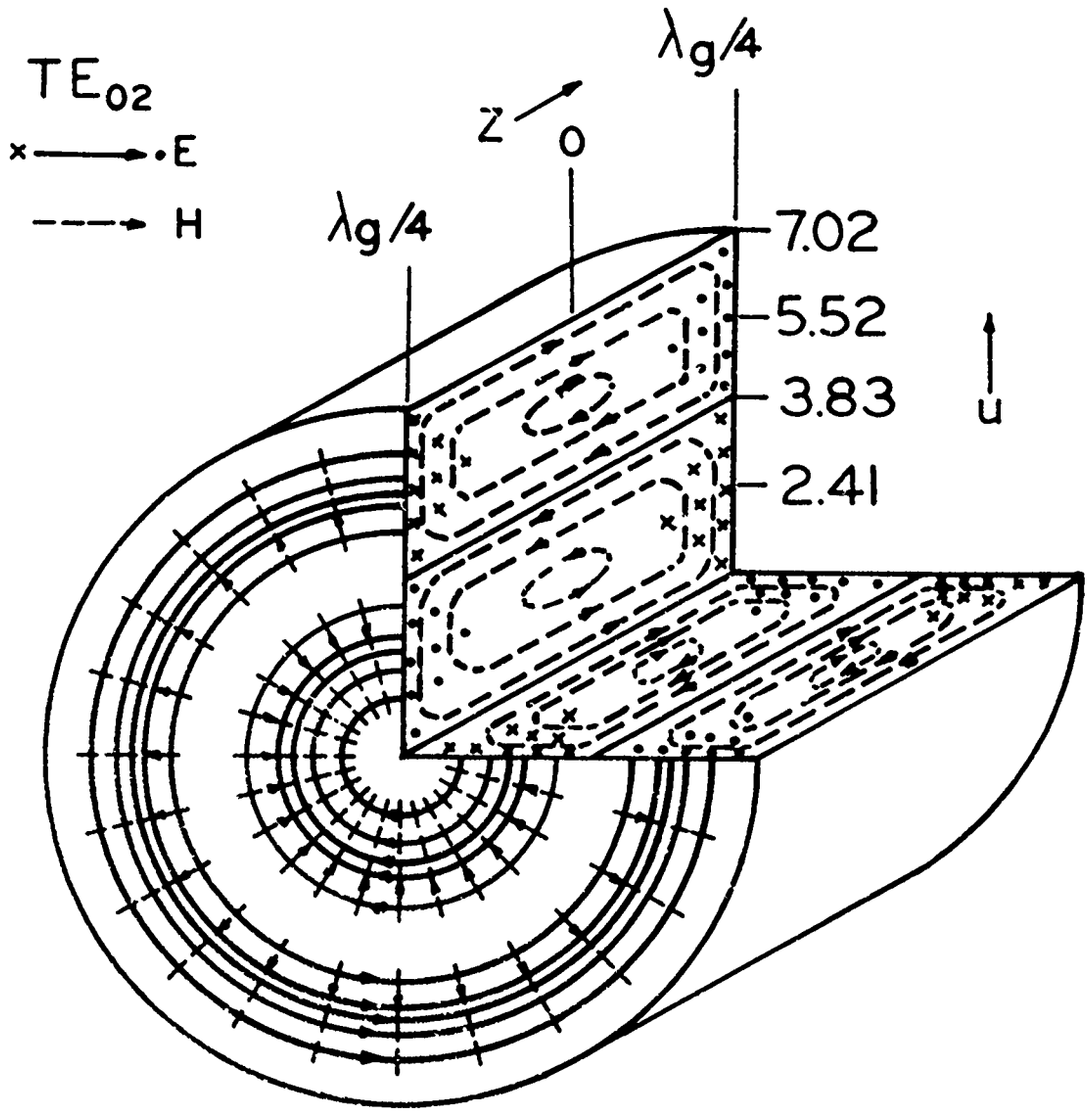

FIG.3

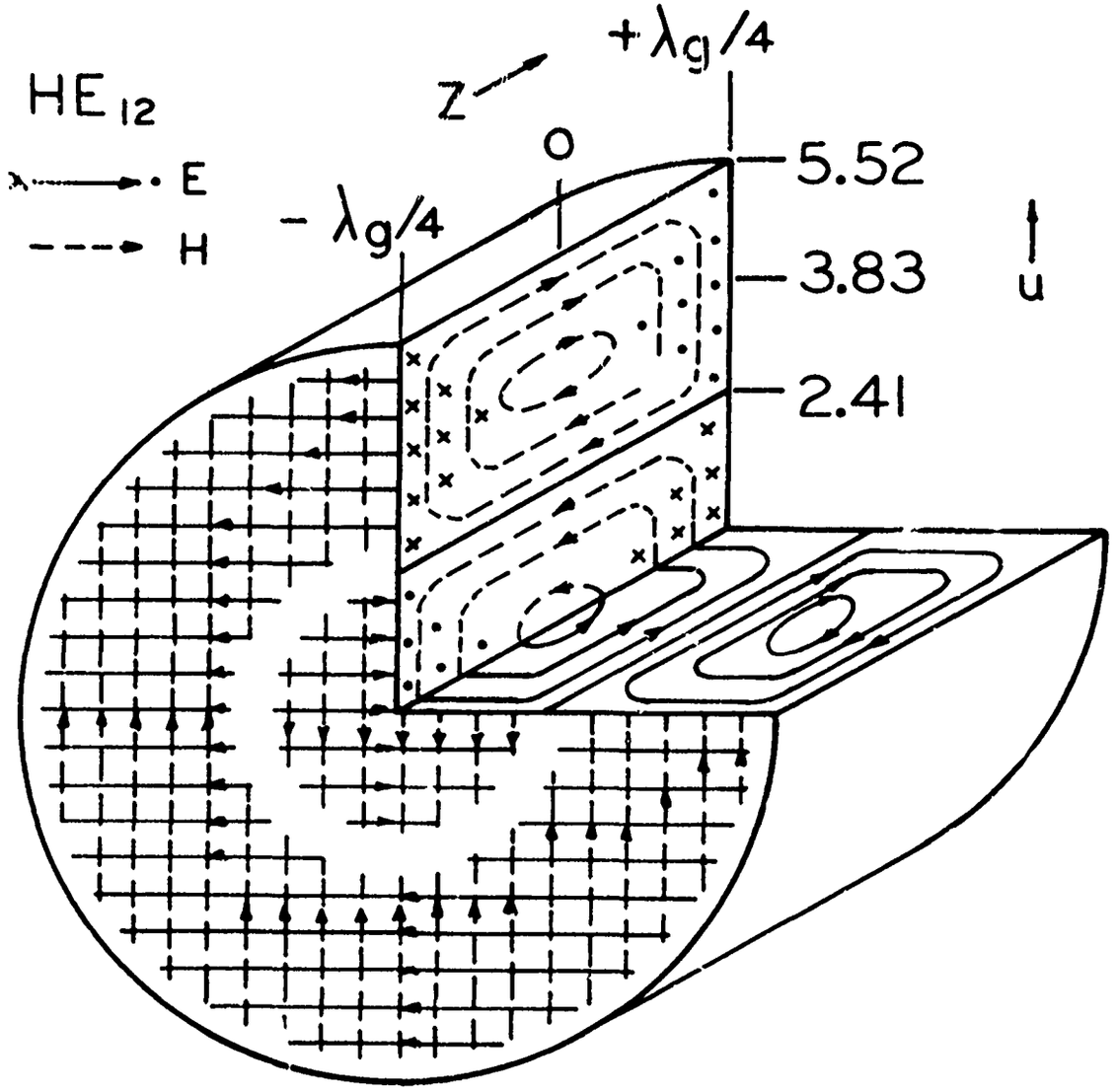

FIG. 4

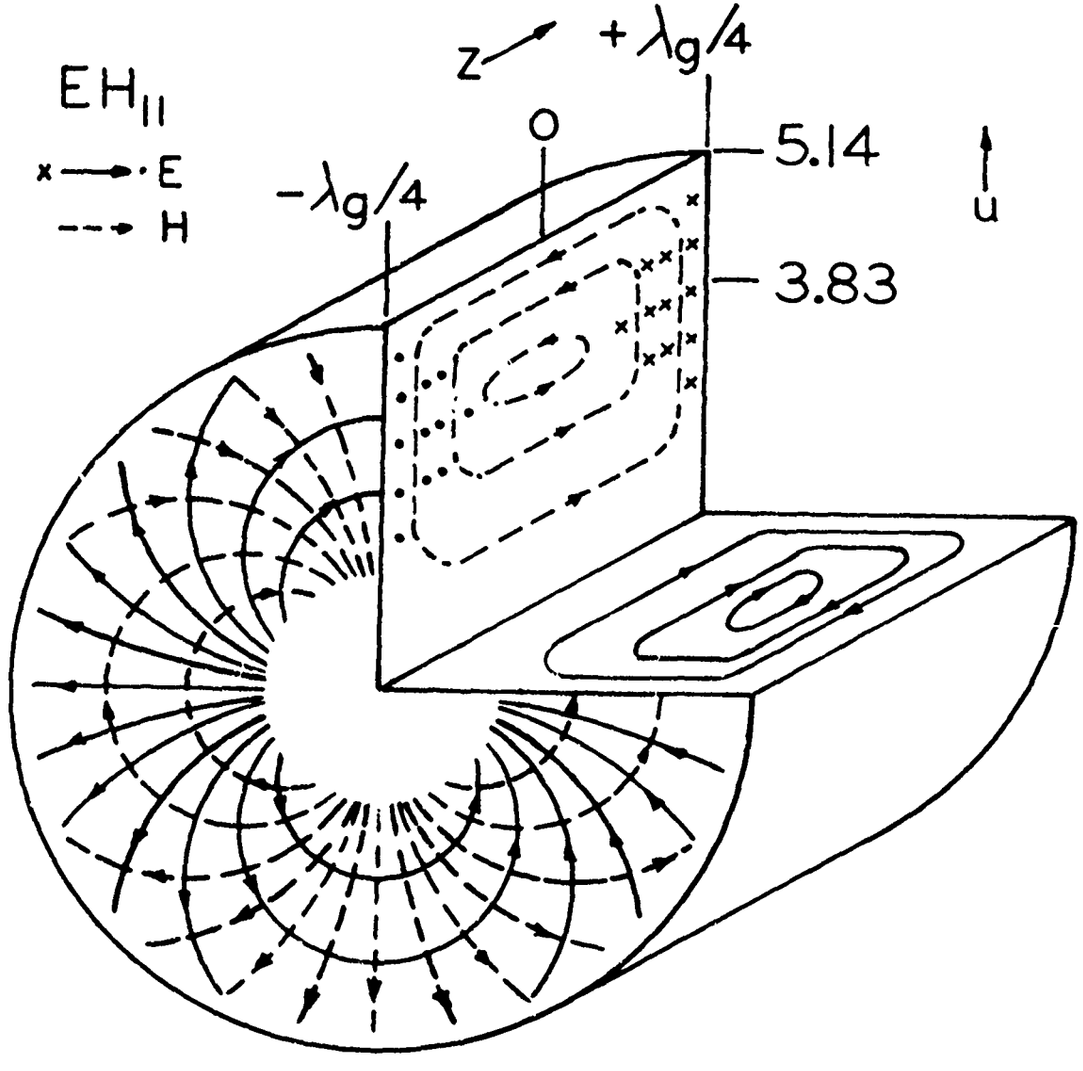

FIG. 5

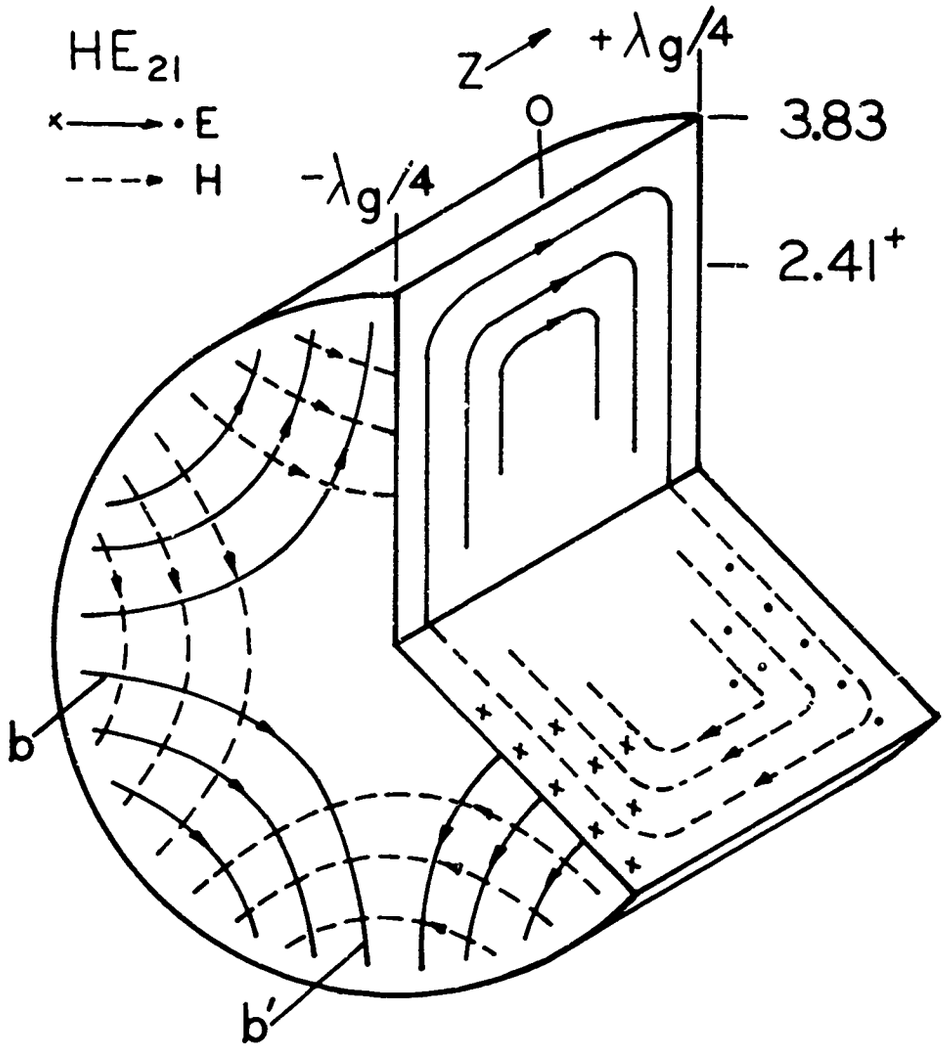

HYPERBOLIC SECTION b-b'

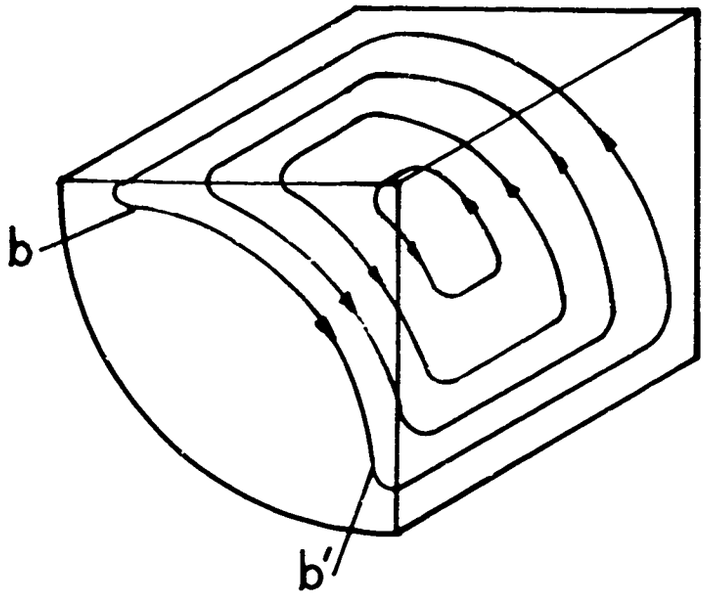

FIG. 6

DISTRIBUTION LIST

Distribution for this Scientific Report is in accordance with the Master Distribution List, List S-S, for the Antenna Laboratory, Electronics Research Directorate, AFCRL, Office of Aerospace Research, U. S. Air Force, Bedford, Massachusetts, which was extant in August 1961.